ELSEVIER

# $^{129}$I and $^{119}$Sn Mössbauer spectroscopy, reversibility window and nanoscale phase separation in binary Ge$_x$Se$_{1-x}$ glasses

P. Boolchand[a],*, P. Chen[a], M. Jin[a], B. Goodman[b], W.J. Bresser[c]

[a]Department of Electrical and Computer Engineering and Computer Science, University of Cincinnati, Cincinnati, OH 45221-0030, USA
[b]Department of Physics, University of Cincinnati, Cincinnati, OH 45221-0011, USA
[c]Department of Physics and Geology, Northern Kentucky University, 143 Natural Science Center, Nunn Drive, Highland Heights, KY 41099, USA

## Abstract

The molecular structure of the prototypical chalcogenide glass system—Ge$_x$Se$_{1-x}$ in the $0 < x < \frac{1}{3}$ range, has received much scrutiny over the years. These glasses have been probed by modulated DSC, Raman scattering, $^{119}$Sn absorption and $^{129}$I emission Mössbauer spectroscopy, and neutron scattering. The $^{129}$I measurements utilize $^{129m}$Te parent as a dopant in glasses, and reveal a bimodal (A, B) distribution of sites, with the site intensity ratio, $I_B/I_A$ ($x$), tracking changes in glass structure as a function of $x$. At low $x$ ($<0.15$) Se$_n$-chains are *stochastically* cross-linked by Ge additive, and $I_B/I_A$ ($x$) sharply declines with $x$. But at $x > 0.15$, rigid regions nucleate at the expense of floppy ones, and the ratio $I_B/I_A$ ($x$) reverses slope to display a global maximum in the $0.20 < x < 0.25$ range. The latter coincides with the reversibility window usually taken as signature of *self-organization* of these networks. At $x > 0.26$, these glasses enter a stressed-rigid elastic phase and in the $0.31 < x < \frac{1}{3}$ range nanoscale phase separate into Se-rich and Ge-rich regions. The signature of the latter is saturation of $I_B/I_A$ ($x$) at a high value of 1.5 at $x = \frac{1}{3}$. $^{119}$Sn Mössbauer spectroscopy measurements independently support the picture of broken chemical order of the stoichiometric glass inferred from the $^{129}$I Mössbauer experiments. These observations using local probes are well correlated to Raman scattering, modulated differential scanning calorimetric and diffraction measurements.
© 2006 Elsevier B.V. All rights reserved.

*PACS:* 61.40.Fs; 63.50.+x; 78.30.Ly; 76.80.+y

*Keywords:* Mössbauer spectroscopy; Raman scattering; Modulated DSC; Self-organization; Nanoscale phase separation

## 1. Local probes of condensed matter

On this occasion of the 35th anniversary of Hyperfine Interactions at La Plata, it is timely to reminiscence on the role played by local probes of condensed matter since their inception. Mössbauer spectroscopy (MS), nuclear quadrupole resonance (NQR), nuclear magnetic resonance (NMR), Perturbed angular correlations (PAC) in its time differential and integral variant, each has had a profound impact on basic materials research. Soon after the discovery of the Mössbauer effect [1] a pivotal step in the field was understanding the magnetic hyperfine structure in α-Fe. S.S. Hanna and collaborators, in several pioneering contributions [2,3], showed how the internal magnetic field

and g-factor ratio of the nuclear ground and excited state in $^{57}$Fe serve to uniquely fix the 6-line nuclear Zeeman spectrum in a Mössbauer experiment. In the next four decades, magnetic materials were probed with unparalleled precision [4–6]. Crucial insights into understanding magnetically ordered as well as disordered solids including spin-glasses became possible as *bulk* magnetization experiments using traditional magnetometers were complemented by *microscopic* magnetization measurements using both MS and PAC.

In a parallel fashion, investigations of quadrupolar hyperfine interactions using either nuclear ground states (NGR), or nuclear excited states (MS, TDPAC), made possible measurements of electric field gradients (EFGs) in non-cubic crystalline solids. And since these extranuclear fields are most sensitive to distribution of valence electrons of probe atoms, issues such as local coordination of atoms,

*Corresponding author. Tel.: +1 513 556 4758; fax: +1 513 556 4790.
*E-mail address:* pboolcha@ececs.uc.edu (P. Boolchand).

and particularly their departure from cubic symmetry could be probed with elegance. MS studies offered a particular advantage over other hyperfine interaction probes; one could access *both* the local structures as well as the local vibrational density of states of substituent atoms or guest atoms in crystalline solids. Starting in the mid- 1970s, $^{129}$I MS [6,7] evolved into a powerful probe of chalcogen sites in crystalline solids, and subsequently in non-crystalline solids. The attractive properties of the 27.8 keV gamma transition in $^{129}$I using the $\frac{5}{2}$ excited and $\frac{7}{2}$ NGS (weakly radioactive) have included [7] the narrow emission linewidth, large nuclear quadrupole moments of the states involved, and the reasonably long half life (33 d) of the $^{129m}$Te parent. The absence of a suitable nucleus possessing a finite ground state quadrupole moment amongst the chalcogens (S, Se, Te) has precluded the use of traditional NQR experiments on chalcogenides. Furthermore, in noncrystalline solids, it has emerged, that local arrangements of atoms are, in general, rather well defined even though long-range structure is absent. The finding goes back to the idea of J.C. Phillips that glass formation in network systems is promoted largely because of a hierarchical nature of valence bond forces [8]. The strong valence forces between nearest neighbors serve as rigidity determining (Lagrangian) constraints. In chalcogens, which have an open "p" valence shell, the primary source of EFGs is these same valence electrons. It is for this reason that EFGs are closely correlated to local coordination and can be used to tag local environments of various atomic species in a solid. In contrast, although direct methods using diffraction have worked well in understanding the structure of crystalline solids, they have limitations for extracting details of atomic scale structure in non-crystalline solids [9]. These limitations are particularly severe for extracting PDF of multi-component atomic systems; and modeling their structures [10] can be a challenge.

As a consequence, local probes of glass structure have had an enormous impact in understanding the disordered state of matter. One can not only deduce aspects of local atomic structure [11] from the measured EFGs, but as experiments have revealed, in favorable instances even aspects of medium range structure from variations of site integrated intensity ratios [12] as a function of glass composition. As these investigations evolved, one came to recognize that the fashionable *chemically ordered continuous random network (CRN) structure of silica*, first introduced by W.H. Zachariasen [13] in 1932, was really the exception rather than the rule. In this context the term continuous refers to networks that are fully polymerized. Structure studies on chalcogenide glasses have revealed that their networks are rarely random [14], or chemically ordered [14], or continuous [15] even at stoichiometric compositions. In more recent years, detailed studies of these systems over a parameter range of network connectedness as defined by the mean coordination number, $r$, have provided evidence [16–21] of a nearly discontinuous

transition to a new topological phase in the vicinity of $r \sim 2.4$ with unusual functionalities. The structural backbones of glasses in this phase are intrinsically stress-free in character, and aging behavior is suppressed [22,23]. These recent findings have emerged largely from Raman scattering and modulated DSC measurements [20–24]. Some indication that an intermediate phase should exist around $r = 2.4$ is provided by the numerical simulations of self-organized networks by Thorpe et al. [18], but its unusual functionalities were not anticipated.

Similarly, the molecular structure of binary $Ge_xSe_{1-x}$ glasses was investigated [25] in considerable detail by $^{129}$I MS in 1986 before the existence of the intermediate phase in these glasses was recognized. In this work, we revisit the $^{129}$I MS measurements of 1981 and 1986, and discuss their significance in relation to the intermediate phase, self-organization effects and nanoscale phase separation (NSPS) in these glasses, ideas that have evolved in the field only during the last six years.

## 2. Morphological structure of stoichiometric GeSe$_2$ glass

Interest in inorganic glasses based on the oxides and chalcogenides of the group III–V elements emerged in the early 1960s. Applications of the chalcogenides evolved with the introduction of the Xerox copier [26] that utilizes a Se-rich film as a photoreceptor, and the discovery of electrical and threshold switching [27] in telluride glasses by S.R. Ovshinsky and collaborators. Silica fibers for optical communication, Ovonic memory devices based on phase change materials [28] and information storage on rewritable DVDs [29] have made use of the glassy state of matter. The issue remains to acquire a more detailed picture of the intermediate range molecular structure in these materials. In this context the concept of constraint counting [8,18,30] has proved to be far more insightful in understanding the functionality of these materials rather than building real space models using balls and sticks as popularly practiced in describing crystalline structures.

### 2.1. $^{129}$I MS

Fig. 1 reproduces the $^{129}$I Mössbauer emission spectrum in the elemental chalcogens along with results on two binary stoichiometric glasses, GeSe$_2$ and GeS$_2$ glasses, taken from the work of Bresser et al. [31] in 1981. In these experiments a *bimodal distribution of sites* is observed in the binary glasses, but a *unimodal one* in the elemental chalcogens. Details of the lineshape analysis and nuclear quadrupole coupling parameters are available in Ref. [12].

Prior to the work of Bresser et al. [31], it was widely believed that stoichiometric GeSe$_2$ glass in analogy to the case of silica, SiO$_2$, also consists of chemically ordered CRN of Se bridging Ge(Se$_{1/2}$)$_4$ tetrahedra [32]. Indeed, if this were the case, one would have expected to observe a single chalcogen site, a Se site having two Ge near neighbors, henceforth labeled as site A. The blue site,
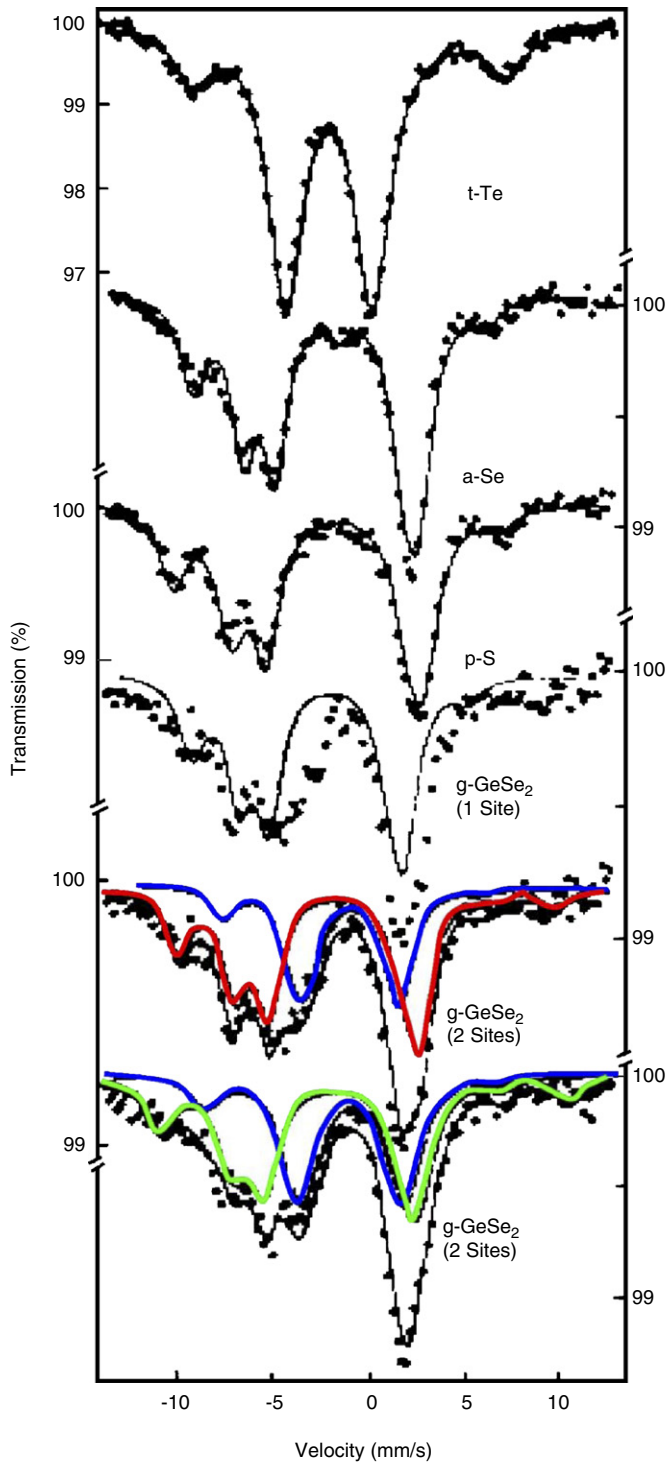
Fig. 1. $^{129}$I Mössbauer emission spectra of c-Te, a-Se and p-S show one I site. Spectra of GeSe$_2$ and GeS$_2$ glasses reveal 2 chemically inequivalent sites. The site common to the binary glasses and colored blue is assigned to I–Ge $\sigma$ bond, while the second site in GeSe$_2$ glass, colored red, is the same as the one in Se glass and it is assigned to I–Se $\sigma$ bond. See Ref. [31] for more details.

common to the spectra of GeSe$_2$ and GeS$_2$ glass, is the site in question. The bimodal distribution (A, B) of parent $^{129}$Te sites in GeSe$_2$ glass showed for the first time that there are two distinct Se local environments, a chemically

ordered Se site A having two Ge near neighbors, and a chemically disordered Se site B having a Se and a Ge near neighbor. Note that the second site (B; colored red) observed in the spectrum of GeSe$_2$ glass is the site also observed in Se glass [33]. And it must, therefore, be identified with a parent Te site having at least a Se neighbor, or in other words, in the glass some Se–Se bonds must occur. But the real surprise of these MS results was that the observed integrated intensity of the *chemically disordered site* to the *chemically ordered one*, $I_B/I_A$, was found to be 1.5 or 150%, unusually high. By examining the variation of $I_B/I_A$ ($x$) in Ge$_x$Se$_{1-x}$ glasses [12,34], it was shown that the Te dopant strongly favors (factor of 75 or more) occupancy of the disordered over the ordered site and that the concentration of Se–Se bonds in the stoichiometric glass is only about 2%. The covalent radius of Te (1.36 A) exceeds that of covalent Se (1.17 A) by nearly 17%. The result of a much higher Te occupancy of the *disordered over the ordered Se sites* suggested, in a natural way, that there must be a larger *free volume* associated with these sites over the ordered ones, i.e., the glass network structure must be *intrinsically heterogeneous*. This circumstance would then make it possible for the oversized Te probe to select the former B sites over the later A sites and minimize strain energy of the alloyed glass. A specific model of the glass consisting of the disordered Se sites dressing surfaces or edges of characteristic clusters had been proposed by J.C. Phillips [35], and provided an appropriate framework to understand the intrinsically heterogeneous morphological structure of the chalcogenide glass. We shall return to discuss the issue later in Section 4. Detailed diffraction measurements on liquid GeSe$_2$ in 1990, and glassy GeSe$_2$ in 2000, subsequently confirmed the existence of the small but finite concentration of homopolar bonds but only when the full power of isostopic substitution was brought to bear on measurements of the partial distribution functions (PDFs). In spite of these efforts, the diffraction measurements could not address the issue of either the free volume distribution in glass structure or whether these homopolar bonds are segregated or randomly distributed in the glass network structure. Fortunately, these issues were addressed by modulated differential scanning calorimetry (MDSC) as will be discussed next. The pivotal steps in decoding the structure of the glass appear in Table 1. Aspects of chemical order of GeSe$_2$ glass are more easily addressed by local methods rather than diffraction, largely because the degree of broken chemical order here is small ($\sim$2%), and at the limit of detection for diffraction but not for local methods.

### 2.2. $^{119}$Sn MS

If there is a finite concentration of Se–Se bonds in a GeSe$_2$ glass, stoichiometric considerations require that there be an equivalent concentration of Ge–Ge bonds. By doping traces of the isovalent $^{119}$Sn substituent in GeSe$_2$ glass, Mössbauer experiments with the 23.8 keV gamma

Table 1
Historical steps in decoding molecular structure of GeSe$_2$ glass

| Year | Method | Principal structure findings related to GeSe$_2$ glass | Ref. |
|------|--------|--------------------------------------------------------|------|
| 1977 | Neutron and Raman scattering | Support for a chemicallly ordered continuous random network (COCRN) | Nemanich et al. [32] |
| 1977 | Raman and IR reflectance | Mode at $180\,cm^{-1}$ in GeSe$_2$ glass identified with Ge–Ge bonds as in ethane-like Ge$_2$Se$_6$ units | Lucovsky et al. [39] |
| 1979 | Raman scattering | $A_1^c$ Companion mode—Cluster Edge mode; Glass seen as partially polymerized and made up of Ge-rich and Se-rich regions | Bridenbaugh et al. [35] |
| 1981 | $^{129}$I Mössbauer effect | Chemical order of glass network Intrinsically Broken. Glass structure consist of Ge-rich and Se-rich clusters | Bresser et al. [31] |
| 1982 | $^{119}$Sn Mössbauer effect | Ge chemical order intrinsically broken. Fraction of Ge–Ge bonds to Ge–Se bonds near 2%. | Boolchand et al. [40] |
| 1983 | Raman scattering | $A_1^c$ mode identified as mode of an ES tetrahedra; Mode at $217\,cm^{-1}$ identified as cluster- edge Se–Se mode; Glass structure viewed as having a small concentration of Ge–Ge and Se–Se bonds | Murase [41] |
| 1991 | Neutron scattering | PDF measured; liquid GeSe$_2$ structure viewed as composed of a finite concentration of homopolar bonds | Penfold and Salmon [42] |
| 2000 | Neutron scattering | PDFs measured. Confirm GeSe$_2$ glass possesses a 2–3% of homopolar (Ge–Ge, Se–Se) bonds | Petri et al. [43] |
| 2000 | Raman, Mössbauer MDSC | $T_g$ variation in Ge$_x$Se$_{1-x}$ glasses show Ge–Ge bonds first appear near $x{\sim}0.30$ and form part of a separate nanophase. GeSe$_2$ glass viewed to be intrinsically nanoscale phase separated into Ge-rich and Se-rich clusters | Boolchand and Bresser [14] |

rays showed [14] evidence of two chemically inequivalent Sn sites (Fig. 2). One of these, showing a narrow single line, the majority site A corresponds to Sn replacing Ge in a tetrahedrally coordinated Ge(Se$_{1/2}$)$_4$ local structure. The minority site B, showing a doublet, is assigned to Sn replacing Ge in ethane-like Ge$_2$Se$_3$ local structures [36]. The degree of broken chemical order, i.e., ratio of homopolar to heteropolar bonds deduced from these experiments was found to be about 2%, in harmony with diffraction and $^{129}$I MS measurements as discussed elsewhere [12]. There is roughly a factor of 8 enhancement in counting sites over bonds, so that a 2% homopolar bond concentration translates into approximately 16% homopolar site concentration . The intrinsically heterogeneous network structure of GeSe$_2$ glass as composed of large Se-rich and small Ge-rich regions was confirmed from MDSC measurements of the glass transition temperature, $T_g$. Compositional trends in $T_g$ provide important clues on the connectedness [37,38] of a glass network. In binary Ge$_x$Se$_{1-x}$ glasses, the slope $dT_g/dx$ progressively increases in the $0.10 < x < 0.31$ range as the network becomes more cross-linked as we will discuss later. That trend, however, is sharply reversed [14] when $x > 0.31$, a composition where Raman scattering and independently $^{119}$Sn MS show evidence for nucleation of Ge–Ge bonds in these glasses. These thermal, optical and nuclear measurements, taken together, show unequivocally that Ge–Ge bonds, once nucleated in binary Ge–Se glasses at $x > 0.31$, do *not* form part of the network backbone, and they lower the rate at which $T_g$ increases. Instead these bonds clearly must form part of a separate nanophase [14] whose mean coordination number is less than 2.67. With a further increase in $x$ to $\frac{1}{3}$, $T_g$ acquires a global maximum. Finally, the slope $dT_g/dx = 0$ at the stoichiometric glass composition largely because of a substantial NSPS into Ge-rich and Se-rich nanophases.

## 3. Reversibility windows and self-organization in glassy networks

A glass is characterized by a softening temperature that can be established in a DSC measurement [44] by heating a sample at a specific rate, usually 20 °C/min, and observing an endotherm . Starting in 1995, a more sensitive variant of DSC, also called modulated-DSC or MDSC was introduced by TA instruments [45]. With MDSC, the endotherm, as one passes through $T_g$ can be deconvoluted [23] into two contributions; a reversing and a non reversing heat flow. The deconvolution is made possible by programing a sinusoidal temperature variation (A sin $\omega t$) on the linear ramp ($\Delta T/t$), and deducing the part of the heat flow that tracks the sinusoidal variation using fast-Fourier transform. The part of the heat flow that tracks the $T$ oscillations is called the reversing heat flow [45]. Typical values of the scanning parameters used in these experiments include $A = 1$ °C, $\omega = 2\pi/100$ radians/s, and $\Delta T/t = 3$ °C/ min. The difference signal between the total heat flow and the reversing heat flow, defines the non reversing heat flow. This is illustrated in Fig. 3.
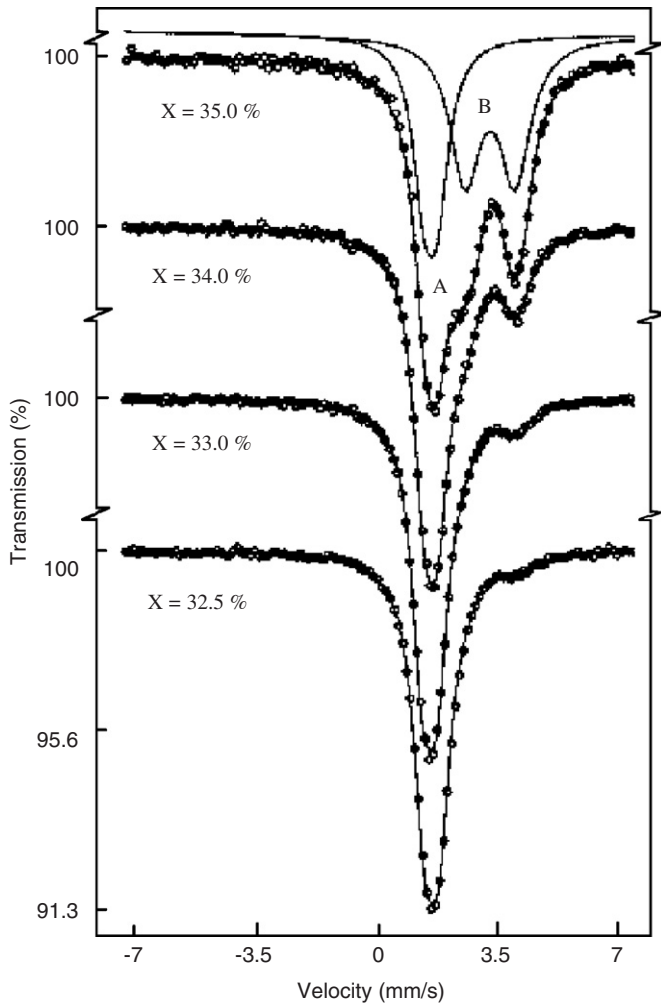
Fig. 2. $^{119}$Sn Mössbauer spectra of $(Ge_{0.99}Sn_{0.01})_xSe_{1-x}$ glasses showing near $x \sim \frac{1}{3}$, presence of two types of chemically inequivalent sites; a single line A site and a doublet B site. See Ref. [14].
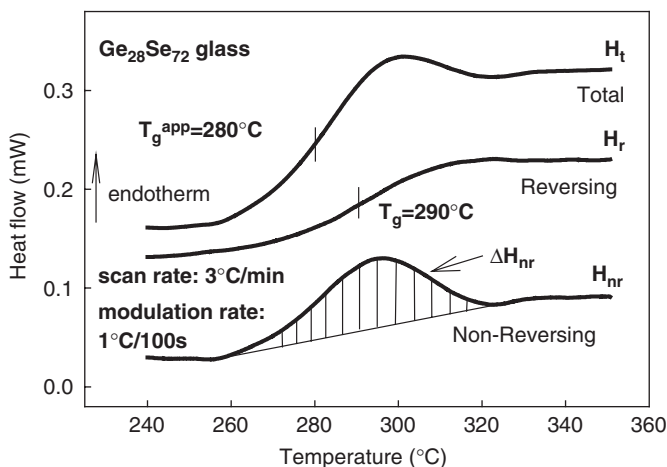
MDSC experiments on a variety of glasses reveal, in general, a reversing heat flow with a characteristic rounded step-like change, while the non reversing heat flow has a Gaussian-like profile shown in Fig. 3 for the case of a $Ge_{28}Se_{72}$ glass [46]. The inflexion point of the reversing heat flow signal is taken to define the glass transition temperature, while the shaded area in Fig. 3 yields the frequency uncorrected non reversing enthalpy, $\Delta H_{nr}$ (up), associated with the melting transition. In these experiments, it is usual to scan up in temperature followed by a scan down in temperature. And the frequency corrected non-reversing enthalpy, $\Delta H_{nr}$, is obtained by taking the difference $\Delta H_{nr}$ (up)$-\Delta H_{nr}$ (down).

There is no rigorous theory for the decomposition shown in Fig. 3, but it is eminently plausible to interpret the reversing component of heat flow as measuring the quasi-equilibrium specific heat of the system as if it were halted at each structural stage of its transition from glass to melt (or the reverse). On the other hand, the non reversing heat flow measures the heat uptake by the system as it passes through the stages of the transition. Aspects of structural arrest, aging and thermal history that characterize the non ergodic character of $T_g$, are all manifested in the non reversing enthalpy [23].

About six years ago, these MDSC experiments on glass systems, performed as a function of network connectedness or mean coordination number, $r$, showed regions near $r \sim 2.4$, for which the $\Delta H_{nr}$ term nearly vanishes [20–24]. In subsequent studies this behavior was recognized as being a universal feature. We call the composition range for these thermally reversing transitions the intermediate phase or reversibility windows. Fig. 4 illustrates the example of a ternary $Ge_xP_xSe_{1-x}$ [22] glass system wherein the reversi-
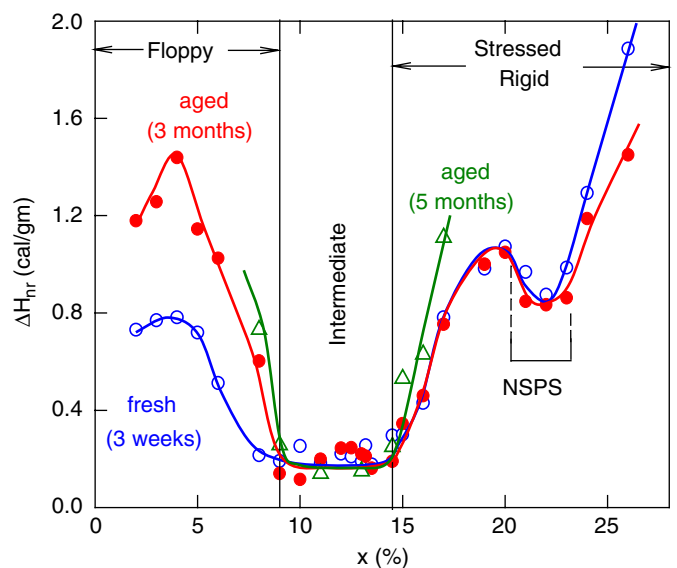


Fig. 3. MDSC scan of titled glass displaying a $T_g = 290\,^\circ C$ from inflexion point of the reversing heat flow, and a non reversing enthalpy, $\Delta H_{nr}$, illustrated by the hash-marked region. The large width $\sim 60\,^\circ C$ of the non reversing heat flow signal is characteristic of networks that are stressed rigid.



Fig. 4. Compositional trends in the non reversing enthalpy, $\Delta H_{nr}(x)$ in ternary $Ge_xP_xSe_{1-2x}$ glasses providing evidence of a reversibility window in the $0.09 < x < 0.145$ range. Also note that glasses in this window do not age, while glass compositions outside this window age. Taken from Chakravarty et al. [22].

bility window is found to occur in the $0.09 < x < 0.145$ range or a mean coordination number range of $2.27 < r < 2.44$. Fig. 4 also shows a profound more recently realized feature of glass compositions in this window, namely, the absence of aging when followed over a period of several months at $T \ll T_g$ [47]. In Fig. 5, we provide a summary of some corresponding results for other glass systems in the form of a bar chart. The length of the bar designates the range of mean $r$ defining reversibility windows. The window in binary $Ge_xSe_{1-x}$ glasses occurs in the $0.20 < x < 0.25$ range, and has been established by detailed compositional studies [46,47]. We shall return to discuss these results in the next section.

We conclude this section with two comments. (i) The connection between thermal properties of glasses discussed above and their elastic behavior has emerged from Raman scattering measurements [24,48,49]. The Raman determined optical elasticity shows different power laws for glass compositions in reversibility windows, and for those outside these windows. The observed power laws are consistent with available numerical simulations [50,51]. The correlation between thermal and optical behavior of the present $Ge_xSe_{1-x}$ glasses places glass compositions at $x < 0.20$ to be in the flexible elastic phase, those in the $0.20 < x < 0.25$ range to the intermediate phase, while those at $x > 0.26$ to the stressed-rigid elastic phase [47,49]. (ii) The two properties, $\Delta H_{nr} \sim 0$ and non aging have been connected with the concept of self-organization of the disordered networks lying in the reversibility window [18]. We cannot go into that concept in any detail. There is however, a purely thermodynamical connection between

the near vanishing of the non reversing heat flow and the absence of aging; Since $\Delta S = S_{melt} - S_{glass} = \int dH_{nr}/T$ where $\Delta T \ll T_g$ is the width of the melting transition, then $\Delta S \sim \Delta H_{nr}/T_g$. Note that the reversing heat flow $H_r$, or specific heat, is not included; thus the change in the vibrational entropy is not counted and $S$ here in the configurational entropy only. Outside the window the values of $\Delta S$ are larger so $S_{glass}$ is smaller there if we assume that $S_{melt}$ does not change dramatically in that range of composition. This means that the entropy of melting is small and that $S_{glass}$ is a maximum for glasses in the window. Now, aging of a system requires it to diffuse over the energy landscape into configurations of higher entropy. These are absent in the window, so the intermediate phase should not age (at least not much).

In the chalcogenides this means the networks for compositions in the intermediate phase are formed from molecular units, so called isostatic units, which link together without incurring energy increasing distortions (or stress). For example, in the $Ge_xSe_{1-x}$ glass system discussed in the following section, the backbone structures are formed from corner sharing (CS) $GeSe_4$ units and ES $GeSe_2$ units. The number of differently linked clusters of nearly the same energy is large and is comparable with the configuration entropy of the liquid. So the large scale isostatic network samples a large number of energetically equivalent configurations over time. This has a direct bearing on the self-organization feature mentioned earlier. In contrast, if the molecular units are made up of stressed units with redundant bonds, there are energy barriers between different configurations and entropy of the network decreases.

## 4. Morphology of binary $Ge_xSe_{1-x}$ glasses, reversibility window and NSPS

Crystalline $Te_xSe_{1-x}$ alloys have been studied [52,53] in X-ray and $^{125}$Te MS studies, and are found to possess a copolymeric structure over the entire $0 < x < 1$ range. Te is isovalent to Se, and both elements belong to the VIth column of the periodic table. Atoms in this column often take on a 2-fold local coordination with two of the 4 valence p-electrons entering into $\sigma$ bonds with nearest-neighbor atoms, and with the remaining two p electrons forming non bonding lone-pairs. It is reasonable to expect Te as an additive in a Se *glass*, to replace Se in the flexible chainlike structure of the non crystalline phase. Upon quenching $^{129m}$Te-bearing Se melts, one expects the Mössbauer parent atom to acquire a bonding configuration characteristic of a chalcogen atom, i.e., chemically bonded to 2 Se near neighbors in a chain. Upon beta decay of the parent atom ($^{129m}$Te), a daughter $^{129}$I is formed, and it will acquire a local bonding configuration characteristic of a halogen. In other words, a bond rearrangement will occur, and a relaxed $^{129}$I–$\sigma$ bond will be formed as the valence decreases by one in going from Te to I. The sign and nuclear quadruple coupling, $e^2qQ$, observed in the $^{129}$I
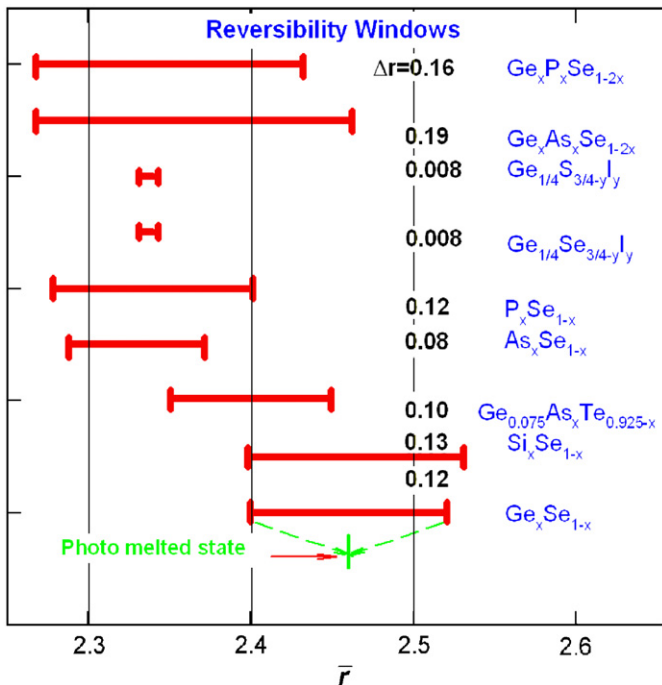


Fig. 5. Observed reversibility windows in indicated glasses from MDSC measurements. In ternary chalcogenide glasses, the window are wide but in chalcohalide glasses they are extremely narrow. See Ref. [47] for details.

Mössbauer experiments confirm the finding as discussed elsewhere [12,33,54]. Henceforth, we shall denote the site formed in a Se-rich glass as the B site.

### 4.1. Why does a CRN description of $Ge_xSe_{1-x}$ glasses fail?

Progressive alloying of Ge into a pure Se glass produces cross-linking of the Se-chains as tetrahedral $GeSe_4$ units emerge at the cross-links. At low Ge concentrations $x$ ($<0.15$), one expects the cross-linking process to result in $GeSe_4$ units that are separated from each other by long $Se_n$-chain links. Up to this point the cross-linking process is stochastic [14,38] but, at $x>0.15$, the relative spacing between the $GeSe_4$ tetrahedra decreases, and in Raman scattering experiments [41,55], both CS and edge-sharing (ES) units emerge. Ultimately, each Se atom serves *as a bridge* between a pair of tetrahedral $Ge(Se_{1/2})_4$ units, and, when $x$ increases to $\frac{1}{3}$, in principle, a completely cross-linked $GeSe_2$ glass could be formed. In a stoichiometric $GeSe_2$ glass that is chemically ordered in this way, one expects $^{129m}$Te to replace Se in a bridging site, and, following nuclear transmutation, to give rise to an $^{129}$I–Ge $\sigma$ bond after a chemical bond rearrangement occurs. Since the half-life ($\sim 16.8$ ns) of the nuclear excited state ($\frac{5}{2}$ state at 27.8 keV) is much longer than the bond rearrangement times ($<10^{-12}$ s), there will be ample time for the daughter atom to acquire a relaxed local environment characteristic of a halogen atom. The site formed in this process is called an A site. If the cross-linking process of Ge with Se were completely stochastic, the resulting $GeSe_2$ glass would be a chemically ordered CRN, and the site concentration ratio, $N_B/N_A(x)$, should steadily decrease [25] from an infinite value at $x=0$, to a vanishing value at $x=\frac{1}{3}$. The expected behavior, namely,

$$N_B/N_A = (1/3 - x)/\lambda + (1/3 - x)^2/4\lambda^2, \qquad (1)$$

is shown in Fig. 6(a) by the dashed curve. Here $\lambda = \exp(-kT_g/\Delta E)$, and the bond energy difference $\Delta E = D(\text{Ge–Te}) + D(\text{Se–Se}) - D(\text{Te–Se}) - D(\text{Ge–Se})$. Here $D(X-Y)$ represents the dissociation energy of the $X-Y$ bond, and the completely random case is $\Delta E = 0$ or $\lambda = 1$.

The observed ratio $I_B/I_A$ $(x)$ of the Mössbauer site integrated intensity appears to track the stochastic variation $(N_B/N_A(x))$ at low $x$ ($<0.15$), but then *deviates qualitatively* as $x>0.15$. A broad maximum near $x = 0.23$ appears and is followed by a rapid saturation at $x>0.31$ to a rather high value of 1.50 (instead of 0) at $x = \frac{1}{3}$. What can we make of these deviations?

### 4.2. The local maximum in $I_B/I_A(x)$ near $x = 0.23$ and the intermediate phase

The broad peak in $I_B/I_A$ $(x)$ centered near $x = 0.23$ coincides with the broad minimum [46,47] of the reversibility window (Fig. 6c), as well as with the broad minimum [56] in molar volumes (Fig. 6b) of these binary glasses. These results unambiguously reveal that the cross-linking
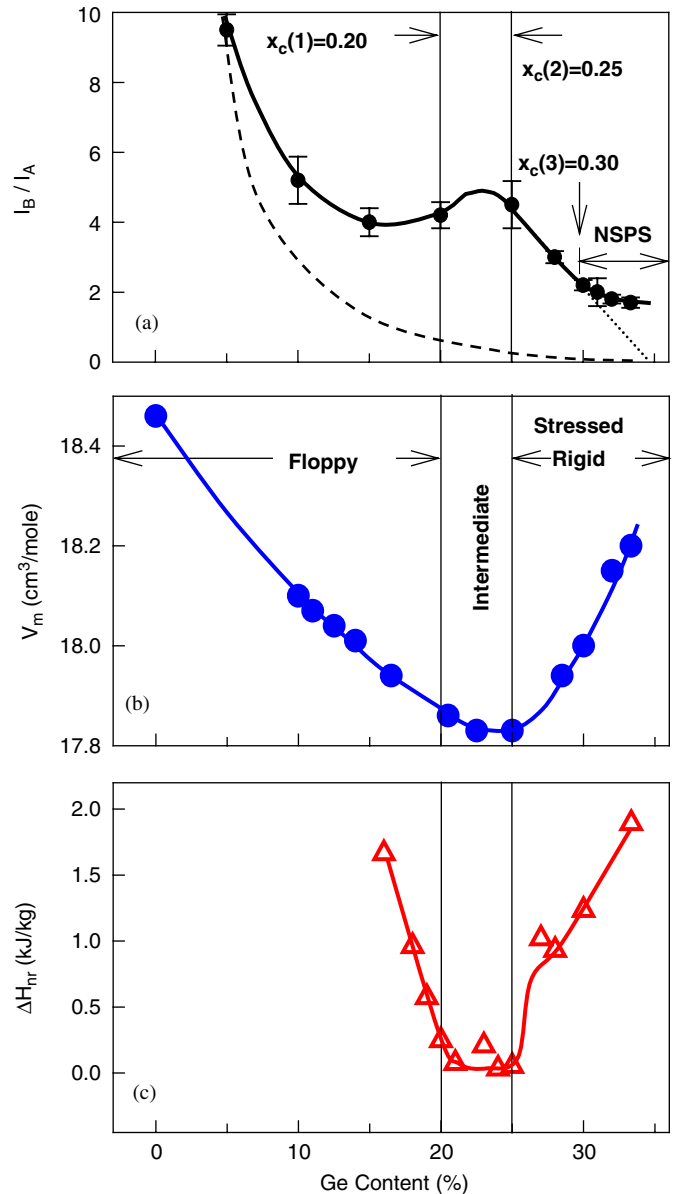


Fig. 6. Variations in (a) $^{129}$I Mössbauer site intensity ratio, $I_B/I_A(x)$, (b) molar volumes and (c) non reversing heat flow, $\Delta H_{nr}(x)$ in binary $Ge_xSe_{1-x}$ glasses. In panel (a) the dashed line gives the variation of the concentration ratio $N_B(x)/N_A$ of these sites based on Eq. (1). The compositional window, $x_c(1) = 0.20 < x < x_c(2) = 0.25$ corresponds to the reversibility window from (c), while $x_c(3) = 0.31$ gives the threshold composition for onset of nanosacale phase separation as discussed in Ref. [14].

of Se chains by Ge additive ceases to be stochastic once $x>0.15$. According to the count of Lagrangian constraints associated with nearest neighbor bond-stretching and bending forces [17], the Se bridging cross-link points between $Ge(Se_{1/2})_4$ tetrahedra are mechanicallly rigid while the Se bridging atoms across Se atoms in a $Se_n$-chain fragments are *mechanically floppy*. The $GeSe_4$ units possess $n_c = 3$ constraints per atom, as required for rigidity while Se–Se–Se chain fragments possess $n_c = 2$ constraints per atom. As the binary glass composition approaches the mean-field rigidity transition [8,57] near $x = 0.20$, rigid

regions composed of CS $GeSe_4$ and ES $GeSe_2$ units come together and percolate. The process results in the oversized Te probe being expelled from the rigid regions to the more flexible regions with Se–Se–Se-chain fragments meeting their bonding requirements without incurring a large increase in strain energy. This expulsion leads to B sites being formed at the expense of A sites, and the ratio, $I_B/I_A(x)$, increases as $x > 0.15$: which is in disagreement with the CRN predicted behavior in Fig. 6a. As $x$ increases beyond 0.25, the ratio $I_B/I_A(x)$ begins to decrease again, largely, because of the reduced concentration of available floppy (Se-rich) regions in the glasses.

## 4.3. Saturation of Mössbauer site intensity ratio $I_B/I_A(x)$ in the $0.31 < x < 0.33$ range and NSPS of $Ge_xSe_{1-x}$ glasses

The second significant feature of Fig. 6a is seen at $x_c(3) = 0.315$. The observed leveling of the $I_B(x)/I_A$ term at larger values of $x$ ($> 0.31$) suggests that the additional Ge is no longer going into the network backbone; and this interpretation is supported by compositional trends in $T_g$. In the $0.31 < x < 0.33$ composition range, the binary glasses are viewed to be nanoscale phase separated into Se-rich and Ge-rich regions. The idea first emerged from a detailed examination of the compositional trends in $T_g$ (Fig. 7b) that revealed the slope $dT_g/dx$ to show a maximum near $x = 0.31$ (Fig. 7c). For convenience of the reader we have reproduced in Fig. 7a, the Mössbauer $^{129}I$ site intensity variation $I_B/I_A(x)$ in the $0.24 < x < 0.34$ range. Note that the steady reduction in $I_B/I_A(x)$ in the composition range $0.24 < x < 0.31$, is followed by a rapid saturation to a value of about 1.50 once $x > 0.31$. The most natural interpretation of this saturation effect is that, once Ge-rich clusters nucleate, a Se-rich cluster must apparently also form. The Se-rich cluster (Fig. 8) is visualized to consist of an interior that is made up of a network of CS and ES units, and whose surfaces are reconstructed to have Se–Se bonds. Fig. 8 provides the structural motif of the layered form ($\alpha$-) of $GeSe_2$. It shows a pair of CS chains joined laterally by ES units, although in the crystalline form there is a repeating structure of such chains as the network is fully polymerized. In glasses, the cluster interior width was estimated earlier at approximately 6 CS chain from the observed degree of broken chemical order in $^{119}Sn$ Mössbauer spectrometry [12]. The cluster edges (Fig. 8) are viewed to have Se–Se bonds which open new surfaces or edge sites and de-polymerize the glass network. The oversized Te probe atoms show a *strong preference* to occupy these surface Se sites, and it is for this reason that the ratio $I_B/I_A$ remains at a high value of 1.5 as $x$ increases to $\frac{1}{3}$. In a chemically ordered CRN model of these glasses, one would have expected the $I_B/I_A$ ratio to linearly decrease to 0 as the dotted line shown in Figs. 6a and 7a. The saturation of $I_B/I_A(x)$ once $x > 0.31$, is consistent with NSPS of these glasses leading to a stoichiometric glass ($GeSe_2$) that is *neither chemically ordered nor fully polymerized* [12,14,35]. The steadily increasing molar
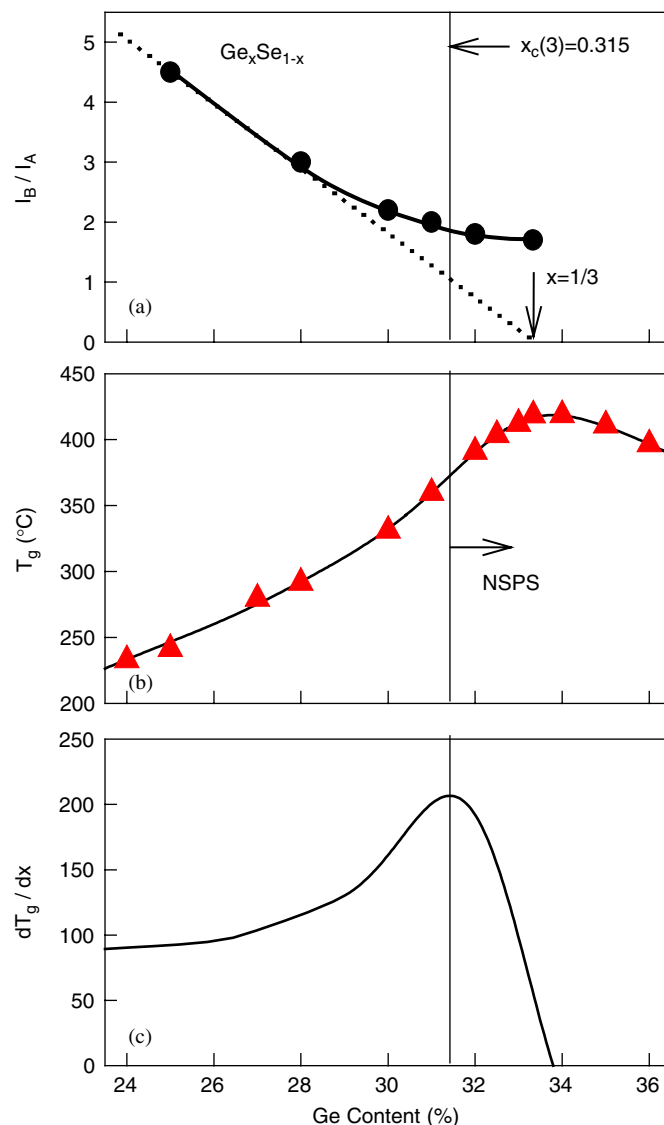


Fig. 7. Variation in (a) $I_B/I_A(x)$ from $^{129}I$ Mössbauer experiments, (b) $T_g(x)$ and (c) $dT_g/dx$ in $Ge_xSe_{1-x}$ glasses in the $0.24 < x < 0.34$ range. Results of panel (a) are taken from Ref. [25], while those of panel (b) and (c) from Ref. [14]. In panel (a) the dotted line would be the expected variation if glasses were to form a chemically ordered CRN.

volume of glasses in the $0.30 < x < \frac{1}{3}$ range (Fig. 6b) with increasing $x$ is in harmony with clustering that opens free volume between clusters due to lone pair (van der Waals) repulsion. In the $0.26 < x < 0.31$ range, the increase of free volume with increasing $x$ is a reflection of the accumulation of network stress [55] due to redundant bonds as discussed elsewhere.

In retrospect, one cannot overemphasize the reward of using $^{129m}Te$ atoms to probe Se environments of stoichiometric $GeSe_2$ glass using MS; the strong preference exhibited by the oversized probe atoms to replace *disordered* Se sites over the *ordered* ones, has led to a pronounced enhancement (factor of 75) of the broken chemical order. Parallel Mössbauer experiments on $As_2Se_3$ glasses also reveal [58] a bimodal distribution of chalcogen sites, suggesting that the stoichiometric glass network is
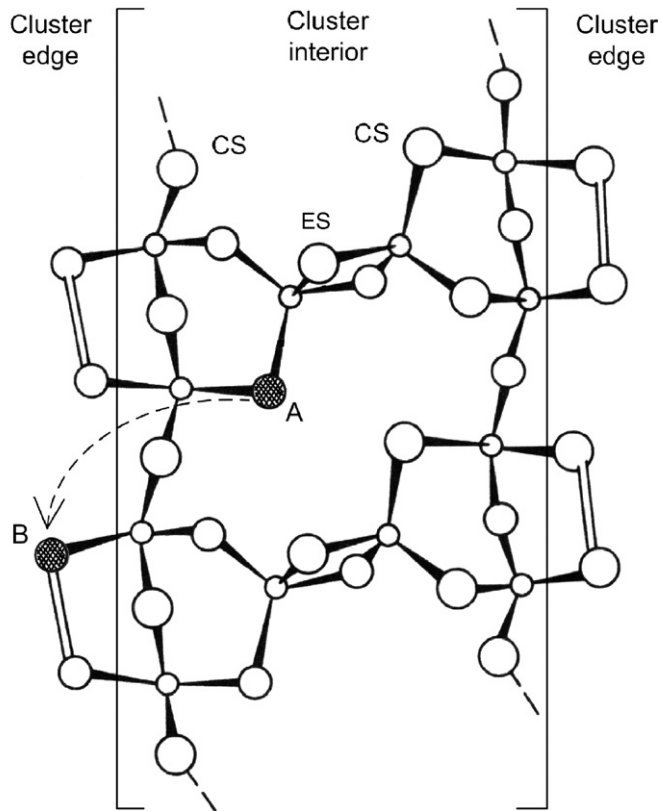
Fig. 8. Two chains ($n = 2$) of corner-sharing (CS) $Ge(Se_{1/2})_4$ tetrahedra separated by pairs of edge sharing (ES) tetrahedra represent the structural motif of $\alpha$-$GeSe_2$. In $GeSe_2$ glass, cluster interior is thought to be made of $n = 6$ chains on an average as suggested in Ref. [12]. The edge reconstruction with Se–Se bonds provides for an internal surface following Ref. [35] thus creating a Se-rich cluster. Expulsion of Te dopant from cluster interior A to cluster edge B chalcogen sites is driven by free energy considerations. The surface segregation of the Te dopant permits lowering strain energy of the Te alloyed $Ge_xSe_{1-x}$ glassy melts by allowing the longer Te–Se bonds to relax in the van der Waals gap. The saturation of the $^{129}I$ Mössbauer site intensity ratio, $I_B/I_A(x)$ in the $0.30 < x < 0.33$ range, along with appearance of Ge–Ge bonds in Raman scattering and $^{119}Sn$ Mössbauer spectroscopy experiments support the notion of an intrinsically nanoscale phase separated structure of these binary glasses into Ge-rich ($Ge_2Se_6$) and Se-rich clusters once $x > 0.30$.

neither fully chemically ordered nor fully polymerized. The finding is consistent with a maximum of $T_g$ near $y = \frac{2}{5}$ [59]. In this respect, the use of substituent atoms, such as $^{75}As$ in NQR or $^{77}Se$ in NMR [60] in probing these aspects of broken chemical order of the stoichiometric glass would lead, understandably, to much smaller effects (a few percent) reflecting their intrinsic concentrations. Furthermore, the success of such local probe experiments requires, in general, that the extra-nuclear fields at the sites in question be different enough to result in hyperfine structures that are easily resolved in the observed lineshapes. In this respect, the case of $As_xSe_{1-x}$ glasses examined recently in $^{75}As$ NQR measurements [61] appears to be a marginal case.

The measured neutron structure factors of $GeSe_2$ glass [9] have been analyzed using first principles molecular dynamic simulations by Massobrio et al. [10], and

independently by Drabold et al. [62]. These groups have also attempted to understand the origin of the first sharp diffraction peak although the issue continues to be a matter of debate. The computational times (approximately 1000 steps of a pico second each) used in equilibrating simulated networks are far too short (by 9 orders of magnitude), and lead to the freezing in of a sizable fraction of Ge and Se atoms that do not conform to the 8-N bonding rule [9]. To circumvent these limitations, an experimentally constrained molecular relaxation (ECMR) method has been proposed [63] which folds in some of the constraints on local coordination numbers imposed by experiments. It is of interest to explore if these new developments in theory will permit bringing the structure of the stoichiometric glass inferred from diffraction experiments closer to the NSPS model deduced from MDSC, Raman scattering and MS experiments.

## 5. Pronounced NSPS in obliquely deposited amorphous $GeSe_2$ thin films

Interest in obliquely deposited amorphous thin films of the chalcogenide was stimulated by the discovery of giant photocontraction effects in such films by K.L. Chopra et al. [64]. Recently, we have examined [65] the molecular structure of amorphous $GeSe_2$ thin films as a function of obliqueness angle $\alpha$ in Raman scattering experiments using 647 nm (1.96 eV) radiation from a Kr-ion laser. The radiation is nearly resonant with the band gap of $GeSe_2$ glass ($E_g \sim 2$ eV) and leads to pronounced scattering. Normally deposited ($\alpha = 0$) films yield Raman lineshapes that are strikingly similar to those of the bulk glass as shown in Fig. 9. The result merely serves as a check on the vapor deposition process. In both cases, lineshapes are dominated by modes of CS- and ES-$Ge(Se_{1/2})_4$ tetrahedra at 200 and 217 cm$^{-1}$, respectively, with relatively weaker features present near 180 cm$^{-1}$ due to Ge–Ge bonds and near 247 cm$^{-1}$ due to Se–Se bonds. The feature near 180 cm$^{-1}$ represents a normal mode of an ethane-like $Ge_2(Se_{1/2})_6$ units [39]. The features at 180 and at 247 cm$^{-1}$ contribute to NSPS of the glass. Raman scattering of obliquely deposited thin films, examined as a function of obliqueness angle, reveal a rather striking evolution of lineshapes that reflects progressive NSPS with increasing $\alpha$. In particular, obliquely deposited thin-films at $\alpha = 80°$ are composed of a columnar structure and are porous [65]. In such films, the network backbone (Fig. 9) is now composed of approximately $Ge_{25}Se_{75}$ stoichiometry comprising the material present in the columns, while the Ge-rich nanophase of $Ge_2Se_3$ stoichiometry forms in between the columns. The underlying NSPS can be qualitatively described by the following relation:

$$GeSe_2 = GeSe_3 + Ge_2Se_3. \qquad (2)$$

The deconvolution of the lineshape for the spectrum of the $\alpha = 80°$ film is illustrated in Fig. 9. The scattering from the Ge-rich nanophase is much weaker than the Se-rich phase
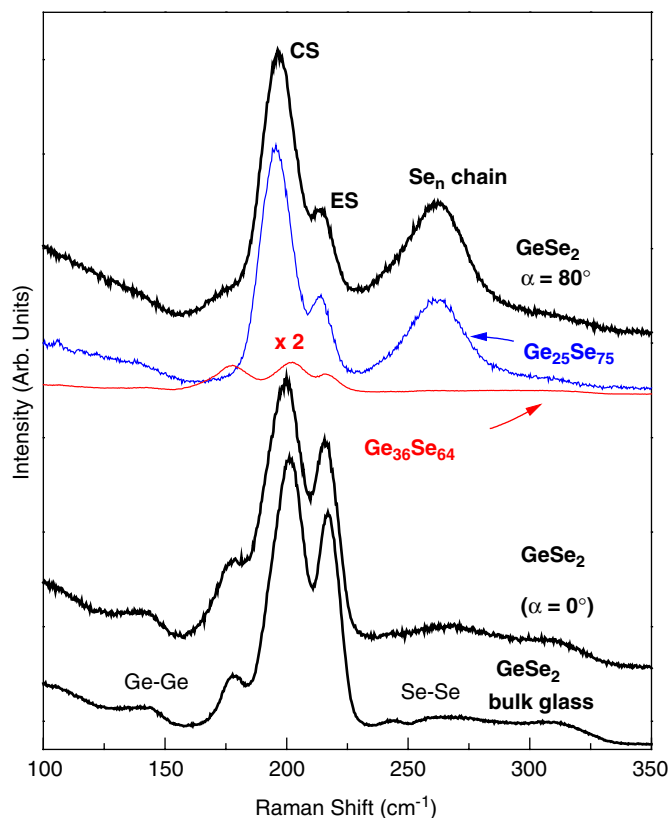
Fig. 9. Raman scattering of $GeSe_2$ bulk glass (bottom), normally deposited amorphous film ($\alpha = 0$) (middle), and obliquely deposited, $\alpha = 80°$, film (top). The principal modes are identified as CS, ES tetrahedra, and Se-chain mode. Lineshape of the obliquely deposited film is deconvoluted in terms of the observed lineshape of $GeSe_3$ glass, and $Ge_{36}Se_{64}$ glass. The scattering cross-section of the Se-rich phase is a factor of approximately 20 more than the Ge-rich phase.

(Eq. (2)), because the band gap associated with Ge-rich phase is smaller, resulting in a loss of resonant Raman scattering. Such NSPS provides a sound basis to understand compositional trends in photocontraction [65] of the obliquely deposited films that is optimized in the reversibility window.

## 6. Conclusion

Crucial insights into the molecular structure of binary $Ge_xSe_{1-x}$ glasses have emerged from modulated differential scanning calorimetry, Raman scattering, $^{119}Sn$ and $^{129}I$ Mössbauer spectroscopy (MS). These experimental probes not only track the onset of rigidity transition at $x_c(1) = 0.20$, but also the onset of nanoscale phase separation near $x_c(3) = 0.31$, and lead to a picture of $GeSe_2$ glass that is intrinsically segregated into Se-rich and Ge-rich clusters. In this respect, the local method (MS), which makes use of an oversized chalcogen ($^{129m}Te$) atom to probe available Se sites in the glasses, reveals that the chemically disordered Se sites possess a *larger* free volume than the ordered Se ones. The result is consistent with the disordered (ordered) Se sites dressing surfaces (interior) of Se-rich clusters. $^{119}Sn$ MS reveals non tetrahedral Sn(Ge)

sites identified with presence of Ge–Ge bonds characteristic of the Ge-rich cluster. These structure findings deduced from thermal, optical and nuclear methods significantly extend those inferred from diffraction methods, and suggest that $GeSe_2$ glass neither forms a continuous nor a chemically ordered random network structure of $Ge(Se_{1/2})_4$ terahedral units. These structural findings on a stoichiometric chalcogenide glass are in sharp contrast to the monolithic structure of the isovalent $SiO_2$ glass, often described as the Zachariasen glass [13].

## References

[1] R.L. Mössbauer, Naturwissenschaften 45 (1958) 538.
[2] S.S. Hanna, J. Heberle, C. Littlejohn, G.J. Perlow, R.S. Preston, D.H. Vincent, Phys. Rev. Lett. 4 (1960) 177.
[3] S.S. Hanna, J. Heberle, G.J. Perlow, R.S. Preston, D.H. Vincent, Phys. Rev. Lett. 4 (1960) 513.
[4] A. SlawskaWaniewska, J.M. Greneche, Phys. Rev. B 56 (1997) R8491.
[5] G.J. Long, D. Hautot, F. Grandjean, D.T. Morelli, G.P. Meisner, Phys. Rev. B 60 (1999) 7410.
[6] S. Jha, R. Segnan, G. Lang, Phys. Rev. 128 (1962) 1160.
[7] H. deWaard, $^{129}I$ Mössbauer spectroscopy, in: J.E. Stevens, V.E. Stevens (Eds.), Mössbauer Effect Data Index covering 1973 Literature, Plenum, New York, 1975, p. 447.
[8] J.C. Phillips, J. Non-Cryst. Solids 34 (1979) 153.
[9] P.S. Salmon, I. Petri, J. Phys: Condens. Matter 15 (2003) S1509.
[10] C. Massobrio, M. Celino, A. Pasquarello, J. Phys: Condens. Matter 15 (2003) S1537.
[11] P. Boolchand, B.B. Triplett, S.S. Hanna, J.P. deNeufville, Mössbauer Spectroscopy of $Te^{125}$, in: J. Gruverman, C.W. Seidel, D.K. Dieterlyvol (Eds.), Some New Results and Applications in Mössbauer Effect Methodology, Plenum, New York, 1974 pp. 9, 53.
[12] P. Boolchand, Mössbauer Spectroscopy—a rewarding probe of morphological structurer of semiconducting glasses, in: D. Adler, B.B. Schwartz, M.C. Steele (Eds.), Physical Properties of Amorphous Materials, Plenum Press, New York, 1985.
[13] W.H. Zachariasen, J. Am. Chem. Soc. 54 (1932) 3841.
[14] P. Boolchand, W.J. Bresser, Philos. Mag. B 80 (2000) 1757.
[15] D.G. Georgiev, P. Boolchand, K.A. Jackson, Philos. Mag. 83 (2003) 2941.
[16] P. Boolchand, D.G. Georgiev, B. Goodman, J. Optoelectron. Adv. Mater. 3 (2001) 703.
[17] P. Boolchand, G. Lucovsky, J.C. Phillips, M.F. Thorpe, Philos. Mag. 85 (2005) 3823.
[18] M.F. Thorpe, D.J. Jacobs, M.V. Chubynsky, J.C. Phillips, J. Non-Cryst. Solids 266 (2000) 859.
[19] J.C. Phillips, Phys. Rev. Lett. 88 (2002) 216401.

[20] D. Selvanathan, W.J. Bresser, P. Boolchand, Phys. Rev. B 61 (2000) 15061.

[21] D.G. Georgiev, M. Mitkova, P. Boolchand, G. Brunklaus, H. Eckert, M. Micoulaut, Phys. Rev. B 6413 (2001) 134204.

[22] S. Chakravarty, D.G. Georgiev, P. Boolchand, M. Micoulaut, J. Phys: Condens. Matter 17 (2005) L1.

[23] P. Boolchand, D.G. Georgiev, M. Micoulaut, J. Optoelectron. Adv. Mater. 4 (2002) 823.

[24] T. Qu, D.G. Georgiev, P. Boolchand, M. Micoulaut, Mater. Res. Soc. Symp. Proc. 754 (2003) CC8.1.1.

[25] W.J. Bresser, P. Boolchand, P. Suranyi, Phys. Rev. Lett. 56 (1986) 2493.

[26] ⟨http://www.xerox.com/innovation/Storyofxerography.pdf⟩.

[27] S.R. Ovshinsky, Phys. Rev. Lett. 21 (1968) 1450.

[28] S.R. Ovshinsky, Applications of glasses, amorphous and disordered materials, in: P. Boolchand (Ed.), Insulating and Semiconducting Glasses, World Scientific, Singapore, River Edge, NJ, 2000.

[29] T. Matsunaga, N. Yamada, Phys. Rev. B 69 (2004) 104111.

[30] J.C. Phillips, J. Non-Cryst. Solids 43 (1981) 37.

[31] W.J. Bresser, P. Boolchand, P. Suranyi, J.P. deNeufville, Phys. Rev. Lett. 46 (1981) 1689.

[32] R.J. Nemanich, S.A. Solin, G. Lucovsky, Solid State Commun. 21 (1977) 273.

[33] C.S. Kim, P. Boolchand, Phys. Rev. B 19 (1979) 3187.

[34] W. J. Bresser, Ph.D. Thesis, University of Cincinnati, 1986.

[35] P.M. Bridenbaugh, G.P. Espinosa, J.E. Griffiths, J.C. Phillips, J.P. Remeika, Phys. Rev. B 20 (1979) 4140.

[36] K. Jackson, A. Briley, S. Grossman, D.V. Porezag, M.R. Pederson, Phys. Rev. B 60 (1999) R14985.

[37] R. Kerner, G.G. Naumis, J. Phys.: Condens. Matter 12 (2000) 1641.

[38] M. Micoulaut, Eur. Phys. J. B 1 (1998) 277.

[39] G. Lucovsky, R.J. Nemanich, F.L. Galeener, Amorphous and Liquid Semiconductors, in: W.E. Spear (Ed.), Center for Industrial Consultancy and Liason, University of Edinburgh, 1977, p. 130.

[40] P. Boolchand, J. Grothaus, W.J. Bresser, P. Suranyi, Phys. Rev. B 25 (1982) 2975.

[41] K. Murase, Vibrational exciatation in glasses: Raman scattering, in: P. Boolchand (Ed.), Insulating and Semiconducting Glasses, World Scientific, Singapore, River Edge, NJ, 2000.

[42] I.T. Penfold, P.S. Salmon, Phys. Rev. Lett. 67 (1991) 97.

[43] I. Petri, P.S. Salmon, H.E. Fischer, Phys. Rev. Lett. 84 (2000) 2413.

[44] C.A. Angell, Glass formation and the nature of the glass transitions, in: P. Boolchand (Ed.), Insulating and Semiconducting Glasses, World Scientific, Singapore, River Edge, NJ, 2000.

[45] Modulated DSC Compendium, Reprint #TA 210, T.A. Instruments, Inc., New Castle, DE, 1997.

[46] P. Chen, P. Boolchand, unpublished.

[47] F. Wang, S. Mamedov, P. Boolchand, B. Goodman, M. Chandra-sekhar, Phys. Rev. B 71 (2005) 174201.

[48] S. Chakravarty, MS Thesis, University of Cincinnati, 2003.

[49] P. Boolchand, X. Feng, W.J. Bresser, J. Non-Cryst. Solids 293 (2001) 348.

[50] H. He, M.F. Thorpe, Phys. Rev. Lett. 54 (1985) 2107.

[51] D.S. Franzblau, J. Tersoff, Phys. Rev. Lett. 68 (1992) 2172.

[52] P. Boolchand, P. Suranyi, Phys. Rev. B 7 (1973) 57.

[53] E. Grison, J. Chem. Phys. 19 (1951) 1109.

[54] G. Langouche, M.V. Rossum, K.P. Schmidt, R. Coussement, Phys. Rev. B 9 (1974) 848.

[55] X.W. Feng, W.J. Bresser, P. Boolchand, Phys. Rev. Lett. 78 (1997) 4422.

[56] A. Feltz, H. Aust, A. Blayer, J. Non-Cryst. Solids 55 (1983) 179.

[57] M.F. Thorpe, J. Non-Cryst. Solids 57 (1983) 355.

[58] P. Boolchand, W.J. Bresser, P. Suranyi, Hyperfine Interactions 27 (1986) 385.

[59] D.G. Georgiev, P. Boolchand, M. Micoulaut, Phys. Rev. B 62 (2000) R9228.

[60] B. Bureau, J. Troles, M. Le Floch, F. Smektala, J. Lucas, J. Non-Cryst. Solids 326 (2003) 58.

[61] E. Ahn, G.A. Williams, P.C. Taylor, D.G. Georgiev, P. Boolchand, B.E. Schwickert, R.L. Cappelletti, J. Non-Cryst. Solids 299 (2002) 958.

[62] M. Cobb, D.A. Drabold, R.L. Cappelletti, Phys. Rev. B 54 (1996) 12162.

[63] P. Biswas, R. Atta-Fynn, D.A. Drabold, Phys. Rev. B 69 (2004) 195207.

[64] B. Singh, S. Rajagopalan, P.K. Bhat, D.K. Pandya, K.L. Chopra, Solid State Commun. 29 (1979) 167.

[65] M. Jin, P. Chen, P. Boolchand, S. Rajagopalan, K.L. Chopra, unpublished.